

Information rate of a waveguide

Vittorio Giovannetti,¹ Seth Lloyd,^{1,2} Lorenzo Maccone,¹ and Jeffrey H. Shapiro¹

¹*Massachusetts Institute of Technology—Research Laboratory of Electronics, 77 Massachusetts Avenue, Cambridge, Massachusetts 02139, USA*

²*Massachusetts Institute of Technology—Department of Mechanical Engineering, 77 Massachusetts Avenue, Cambridge, Massachusetts 02139, USA*

(Received 16 July 2003; published 13 May 2004)

We calculate the communication capacity of a broadband electromagnetic waveguide as a function of its spatial dimensions and input power. We analyze the two cases in which either all the available modes or only a single directional mode are employed. The results are compared with those for the free-space bosonic channel.

DOI: 10.1103/PhysRevA.69.052310

PACS number(s): 03.67.Hk, 42.50.-p, 84.40.Az

In the analysis of electromagnetic communication channels using quantum information, emphasis has been placed on free-space communication protocols, in which waves propagate unconstrained: a good *summa* of all the obtained results can be found in Refs. [1,2]. Here we will focus on constrained communication lines, such as optical fibers or radio waveguides, in the lossless limit. Although the spatial mode structure for free-space propagation between a pair of apertures has long been understood [3], its near-field modes only approximate the lossless behavior of ideal waveguides. In contrast, since the spatial properties of the waveguide modes are always well defined, we will be able to derive the exact dependence of the information rate on the system parameters, e.g., the power P and the waveguide cross-sectional area A , obtaining results that closely resemble the ones described in Ref. [1,4] for the free-space channel. Moreover, as will be discussed in detail, our derivation resolves some of the open issues connected with the optimization of the multimode communication protocols.

We start by describing the waveguide communication channel in Sec. I and calculate the rate in Sec. II. In particular, Secs. II A and II B are devoted to the regimes of multiple modes and single directional mode, respectively. The discussion and the comparison with prior results are given in Sec. III.

I. THE CHANNEL

Although guided-wave optical communications are normally carried out using dielectric waveguides, metallic waveguides provide a simpler mode structure for deriving the broadband information rate. In the ideal, lossless case that we consider, such waveguides confine the electromagnetic field into a finite region of space by means of perfectly reflecting boundaries. In this paper we will analyze in detail the rectangular cross-section case with transverse spatial dimensions L_1 and L_2 described in Fig. 1, even though the procedure can be readily extended to other configurations. In a hollow waveguide the transverse-electromagnetic modes customarily used in free-space communications do not propagate. They are replaced by the transverse-electric (TE) and the transverse-magnetic (TM) modes in which only the

electric and magnetic terms, respectively, possess null longitudinal components. These modes are characterized by the wave vectors [5]

$$\mathbf{k} = \left(\frac{\pi n_1}{L_1}, \frac{\pi n_2}{L_2}, k_3 \right) \quad \text{with} \quad \begin{cases} n_1, n_2 = 1, 2, \dots & \text{TE} \\ n_1, n_2 = 0, 1, 2, \dots & \text{TM,} \\ (n_1 = n_2 = 0 \text{ excluded}) & \end{cases} \quad (1)$$

where the discretization of the transverse components derives from the boundary conditions at the waveguide walls and where the longitudinal component k_3 is a positive quantity because we are considering only modes propagating from the sender to the receiver. By introducing the transmission time \mathcal{T} (i.e., the time interval in which the sender operates the channel), the longitudinal parameter k_3 can be discretized using periodic boundary conditions. In particular, a mode with wave vector \mathbf{k} bounces off the waveguide walls (see Fig. 1) so that it propagates across the transmission line with a longitudinal speed (group velocity) $c \cos \theta \equiv ck_3/|\mathbf{k}|$. This means that all the photons of that mode used in the transmission can be ideally enclosed in a box of longitudinal length $c\mathcal{T} \cos \theta$: assuming periodic boundary conditions k_3 can be discretized as $2\pi n_3/(c\mathcal{T} \cos \theta)$, with n_3 a positive integer. This relation introduces a nonlinearity in the dependence of the mode frequencies $\omega_{\mathbf{k}}(n_1, n_2, n_3) \equiv c|\mathbf{k}|$ on the parameters n_1 , n_2 , and n_3 , i.e.,

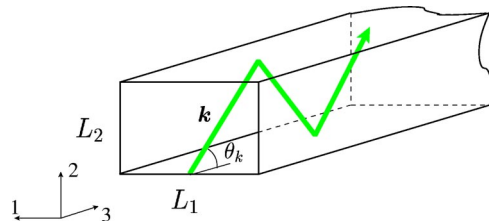


FIG. 1. Description of the ideal metallic waveguide. The modes (TE or TM) with wave vector \mathbf{k} propagate in the positive longitudinal direction bouncing off the perfectly reflecting walls of the waveguide.

$$\frac{\omega_{\mathbf{k}}(n_1, n_2, n_3)}{c} = f\left(\frac{\pi n_1}{L_1}, \frac{\pi n_2}{L_2}, \frac{2\pi n_3}{c\mathcal{T}}\right), \quad (2)$$

where

$$f(\mathbf{x}) \equiv \frac{2(x_1^2 + x_2^2)}{-x_3 + \sqrt{x_3^2 + 4(x_1^2 + x_2^2)}}. \quad (3)$$

As will be discussed in Sec. II A, this is the main difference between our approach and the free-space calculation performed in Ref. [1].

II. THE COMMUNICATION RATE

The communication rate R is the maximum number of bits per second that can be transmitted through the channel, and is given by the capacity (i.e., the maximum of the mutual information between the input and the output of the channel) divided by the transmission time \mathcal{T} . The capacity can be estimated from a quantum-mechanical analysis of the communication in which each symbol θ , transmitted with probability density $p(\theta)$, is associated with a quantum state $\rho(\theta)$ of the Hilbert space \mathcal{H} of the media used in the communication process (in our case, the electromagnetic field). Without any constraints, the infinite dimensions of the input space \mathcal{H} of the system under consideration can accommodate an arbitrary amount of information and the capacity would diverge. Physically it is, thus, sensible to introduce an energy constraint on the accessible input states [2]. In particular, we consider the following limit on the available average power (i.e., energy transmitted per unit time):

$$P = \frac{\text{Tr}[H\rho]}{\mathcal{T}}, \quad (4)$$

where $\rho = \int d\theta p(\theta)\rho(\theta)$ is the average message sent through the channel (i.e., the electromagnetic field state at the input), and H is the Hamiltonian of the modes, i.e.,

$$H = \sum_{\mathbf{k}, \epsilon} H_{\mathbf{k}, \epsilon}, \quad H_{\mathbf{k}, \epsilon} \equiv \hbar \omega_{\mathbf{k}} a_{\mathbf{k}, \epsilon}^\dagger a_{\mathbf{k}, \epsilon}, \quad (5)$$

with $\epsilon = \text{TE, TM}$ and $a_{\mathbf{k}, \epsilon}$ being the annihilation operator of the mode ϵ with wave vector \mathbf{k} and commutator

$$[a_{\mathbf{k}, \epsilon}, a_{\mathbf{k}', \epsilon'}^\dagger] = \delta_{\epsilon\epsilon'} \delta_{\mathbf{k}\mathbf{k}'}. \quad (6)$$

In order to calculate the capacity of the channel under consideration, i.e., the maximization of the mutual information under the constraint (4), we need the infinite-dimensional extension [2] of the Holevo theorem [6] which, in the noiseless case, gives an upper bound to the capacity in terms of the maximal input von Neumann entropy. As discussed in Ref. [2], this upper bound is achievable, so that the rate is

$$R = \max_{\rho} \frac{S(\rho)}{\mathcal{T}}, \quad (7)$$

where $S(\rho) = -\text{Tr}[\rho \log_2 \rho]$ is the von Neumann entropy and the maximum is taken over all the possible density matrices ρ of the modes employed in the transmission, which

satisfy Eq. (4). Notice that Eq. (7) might be seen as an instance of the Holevo-Schumacher-Westmoreland theorem [7], but for the case under consideration it was first derived by Yuen-Ozawa [2]. The maximization of Eq. (7) under the constraint (4) can be performed by means of a variational principle: the maximum is reached for ρ that satisfies

$$\delta \left\{ \frac{S(\rho)}{\mathcal{T}} - \frac{\lambda}{\ln 2} \frac{\text{Tr}[H\rho]}{\mathcal{T}} - \frac{\lambda'}{\ln 2} \text{Tr}[\rho] \right\} = 0, \quad (8)$$

where λ and λ' are the two Lagrange multipliers that derive from the power constraint (4) and from the normalization condition on ρ , respectively (the factor $\ln 2$ has been inserted so that all calculations can be performed using natural logarithms). Using standard techniques (see, for instance, Ref. [8]), it is possible to show that Eq. (8) is satisfied by the density matrix

$$\rho_{\max} = \frac{e^{-\lambda_0 H}}{Z(\lambda_0)}, \quad (9)$$

where $Z(\lambda) \equiv \text{Tr}[e^{-\lambda H}]$ is the partition function and λ_0 is determined by the equation

$$P = - \left. \frac{\partial}{\partial \lambda} \left(\frac{\ln Z(\lambda)}{\mathcal{T}} \right) \right|_{\lambda_0}. \quad (10)$$

Using this solution, the maximum rate in bits per unit time is finally given by

$$R = \frac{1}{\ln 2} \left(\lambda_0 P + \frac{\ln Z(\lambda_0)}{\mathcal{T}} \right). \quad (11)$$

To obtain an explicit expression for R , we thus only need to evaluate the partition function $Z(\lambda)$ for the Hamiltonian (5). In the two following sections we will undertake such endeavor for two different communication scenarios.

A. Multimode communication

In this section we calculate the rate R when all the wave vectors that propagate in the positive longitudinal direction (from the sender to the receiver) are employed in the communication.

Since modes with different \mathbf{k} or different ϵ are independent, the partition function factorizes in product of single-mode partition functions $Z_{\mathbf{k}, \epsilon}(\lambda)$ so that

$$\ln Z(\lambda) = \sum_{\mathbf{k}, \epsilon} \ln Z_{\mathbf{k}, \epsilon}(\lambda), \quad (12)$$

with

$$Z_{\mathbf{k}, \epsilon}(\lambda) \equiv \text{Tr}[e^{-\lambda H_{\mathbf{k}, \epsilon}}] = \frac{1}{1 - e^{-\lambda \hbar \omega_{\mathbf{k}}}}. \quad (13)$$

Substituting Eq. (13) into Eq. (12) one can compute $Z(\lambda)$ by summing over the allowed values of n_1 , n_2 , and n_3 . Since we are interested in the stationary information rate, we should take the limit $\mathcal{T} \rightarrow \infty$ which allows the summation over n_3 to be replaced with an integral. Even with this simplification,

the calculation is quite demanding and is postponed to the final paragraphs of this section for the sake of readability. Here we consider the simpler high-power/high cross-section regime, defined by the condition

$$\gamma \equiv \frac{AP}{c^2 \hbar} \gg 1, \quad (14)$$

where $A=L_1L_2$ is the cross-sectional area of the waveguide. In this regime too, the summations over n_1 and n_2 reduce to integrals and, apart from corrections of order $1/\gamma$, Eq. (12) becomes

$$\ln Z(\lambda) \approx \frac{gAcT}{2\pi^3} \int_V dx \ln \left[\frac{1}{1 - e^{-\lambda \hbar c f(x)}} \right], \quad (15)$$

where the volume integral must be performed on the subspace V of positive x_j and $f(x)$ is defined in Eq. (3). The parameter $g=2$ in Eq. (15) counts the different species of modes, TE and TM in this case. It plays the same role as the polarization degeneracy in the free-space propagation of electromagnetic waves. By performing a change of integration variables and using the integral of Eq. (A2) of the Appendix, Eq. (15) reduces to

$$\ln Z(\lambda) = \frac{g\pi^2}{240} \frac{AT}{\hbar^3 \lambda^3 c^2}. \quad (16)$$

Substituting this result in Eq. (10) gives

$$\lambda_0 = \left(\frac{g\pi^2}{80} \frac{A}{P\hbar^3 c^2} \right)^{1/4}, \quad (17)$$

which through Eq. (11) implies the following maximum rate:

$$R = \frac{4}{3 \ln 2} \left(\frac{g\pi^2}{80} \frac{A}{c^2} \right)^{1/4} \left(\frac{P}{\hbar} \right)^{3/4}. \quad (18)$$

Numerical results. When condition (14) does not apply, the summations over n_1 and n_2 in the definition of $\ln Z(\lambda)$ cannot be performed analytically. In this case we can resort to numerical evaluation of the rate. For the sake of simplicity we will consider a waveguide with square cross section, i.e., $L_1=L_2$. Remembering that not all the values of n_1 and n_2 contribute both to the TE and to the TM modes, the summation of Eq. (12) can be written as

$$\ln Z(\lambda) = \frac{cT}{\sqrt{A}} \mathcal{W} \left(\frac{\pi \lambda \hbar c}{\sqrt{A}} \right) \quad (19)$$

with

$$\mathcal{W}(\beta) \equiv \sum_{n_1, n_2=1}^{\infty} F_{n_1, n_2}(\beta) + \sum_{n_1=1}^{\infty} F_{n_1, 0}(\beta), \quad (20)$$

where

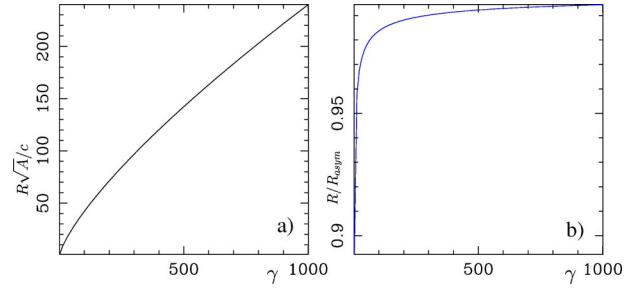


FIG. 2. Numerical plots. (a) Plot of the rate R given by Eq. (22) as a function of the dimensionless parameter γ . (b) Comparison between the same solution and the asymptotic behavior R_{asym} of Eq. (24): the ratio between these two quantities tends to 1 for $\gamma \gg 1$.

$$F_{n_1, n_2}(\beta) \equiv \int_0^\infty dx \ln \left[\frac{1}{1 - e^{-\beta f(n_1, n_2, x)}} \right]. \quad (21)$$

Using Eq. (11), one can show that $R\sqrt{A}/c$ is a function only of the dimensionless parameter γ , defined in Eq. (14). In fact, Eq. (11) becomes

$$R = \frac{c}{\ln 2\sqrt{A}} \left[\frac{\gamma\beta_0}{\pi} + \mathcal{W}(\beta_0) \right], \quad (22)$$

where β_0 is the dimensionless quantity determined by the condition (10), i.e., the solution of

$$\left. \frac{\partial}{\partial \beta} \mathcal{W}(\beta) \right|_{\beta_0} = -\frac{\gamma}{\pi}. \quad (23)$$

In Fig. 2 the numerical evaluation of the rate R is reported. Notice that in the limit $\gamma \gg 1$, the solution (22) approaches the asymptotic behavior

$$\frac{R\sqrt{A}}{c} \rightarrow \frac{4}{3 \ln 2} \left(\frac{g\pi^2}{80} \right)^{1/4} \gamma^{3/4}, \quad (24)$$

which corresponds to the high-power/high cross-sectional limit solution of Eq. (18) discussed previously.

The dimensionless parameter γ that identifies the onset of the asymptotic regime for $R\sqrt{A}/c$ has a relatively simple physical interpretation. From the density matrix, Eq. (9), we see that the occupancy probabilities are highest for the lowest-frequency (lowest photon energy) modes. From the exact formulation for the partition function, Eq. (12), we see that the triple-integral approximation in Eq. (15) will be valid when the occupancy probabilities change very little between modes with adjacent energy levels. The largest such photon-energy spacing occurs for the lowest-frequency modes, and, roughly speaking, is equal to $\hbar c/\sqrt{A}$, i.e., the photon energy of the waveguide's cutoff frequency. If we concentrate all of the sender's average power into the lowest-frequency mode, the resulting power spectral density will be approximately $P\sqrt{A}/c$, and hence γ equals this spectrum measured in units of the photon energy $\hbar c/\sqrt{A}$ of the lowest-order mode. The condition $\gamma \gg 1$ then guarantees the desired smooth behavior of the occupancy probabilities, because Eq. (9) implies that high-photon-number occupancy of the

lowest-order mode will, of necessity, be accompanied by similar occupancy of other low-frequency modes.

This analysis clarifies the regime of applicability of the approximation (18) and underlines the importance of the quantity γ in the definition of maximum rate.

B. Single directional mode communication

In this section we calculate the rate R when the wideband transmission is limited to using a single direction of the wave vector \mathbf{k} . We will specify this direction assigning the polar angle $\theta = \arccos(k_3/|\mathbf{k}|)$ and the azimuth angle $\varphi = \arctan(k_2/k_1)$. In terms of the discretization parameters n_1 , n_2 , and n_3 , these conditions become

$$\frac{n_2}{n_1} = \frac{L_2}{L_1} \tan \varphi, \quad (25)$$

$$\left(\frac{\pi n_1}{L_1}\right)^2 + \left(\frac{\pi n_2}{L_2}\right)^2 = \frac{\sin^2 \theta}{\cos^4 \theta} \left(\frac{2\pi n_3}{cT}\right)^2, \quad (26)$$

where the nonlinear relation of Eq. (2) was used in deriving Eq. (26). In this case, only those modes with \mathbf{k} compatible with the chosen direction contribute to the partition function sum (12), i.e.,

$$\begin{aligned} \ln Z(\lambda) &= \sum_{n_3=0}^{\infty} \sum_{n_1, n_2=1}^{\infty} \ln \left[\frac{1}{1 - e^{-2\pi\lambda n_3/(T \cos^2 \theta)}} \right] \\ &\quad \times \delta_{n_2, n_1 \tan \varphi} \delta_{L_2/L_1} \delta_{n_1, 2n_3 L_1 \sin \theta / [cT(1 + \tan^2 \varphi)^{1/2} \cos^2 \theta]}, \end{aligned} \quad (27)$$

where, for the sake of simplicity, only the TM mode has been considered and where the two Kronecker δ 's take into account the conditions (25) and (26). Again working in the high-power/high cross-sectional regime (14), the summations can be replaced with integrals and the Kronecker δ 's become Dirac δ functions, so that we find

$$\begin{aligned} \ln Z(\lambda) &\simeq \frac{cT}{2\pi} \int_V dx \ln \left[\frac{1}{1 - e^{-\lambda \hbar c x_3 / \cos^2 \theta}} \right] \delta(x_2 - x_1 \tan \varphi) \\ &\quad \times \delta \left(x_1 - x_3 \frac{\sin \theta}{\sqrt{1 + \tan^2 \varphi} \cos^2 \theta} \right) = \frac{\pi T \cos^2 \theta}{12\lambda \hbar}, \end{aligned} \quad (28)$$

where V is again the subspace of positive components of x_j . Substituting this result into Eqs. (10) and (11), we now find that the maximum rate is

$$R = \frac{\cos \theta}{\ln 2} \sqrt{\frac{\pi P}{3\hbar}}. \quad (29)$$

If both the TE and TM modes of the chosen direction were used for the transmission, then a factor $\sqrt{2}$ would appear in Eq. (29).

III. DISCUSSION

In the preceding section we calculated the maximum rate R for information transmission through an ideal metallic

waveguide under an average input power constraint. In particular, we found that when the sender is using all the available modes, R scales as $A^{1/4} P^{3/4}$, as reported in Eq. (18). This scaling is reminiscent of the free-space communication one [1]. The main difference between the two cases is that, for waveguides all the positively propagating \mathbf{k} vectors actually reach the receiver owing to the reflecting walls of the waveguide. For frequency- ω propagation over an L -m-long free-space path between identical circular apertures of diameter D , there are approximately $[D^2 \omega / (8cL)]^2$ low-loss propagation modes per polarization state [3]. In essence, the low-loss modes represent propagation angles that lie within the solid angle subtended by the receiver at the sender. These low-loss modes can be accounted for by introducing a factor of $\sqrt{\sin \theta_{max}}$ (θ_{max} being the channel angular aperture as seen by the sender) in the free-space rate—see Sec. VI A in Ref. [1]. The lossy free-space modes that do not satisfy the preceding angular subtense condition can be used for communication, but their analysis requires inclusion of an accompanying noise source, which is mandated by the quantum theory of loss. As noted at the end of this section, finding the capacity of the lossy propagation channel is a considerably more difficult problem.

Apart from these physical considerations, a technical difference between our calculation and the free-space analysis is also evident. In deriving their result, authors of [1], instead of using Eq. (7), calculate the maximum rate as

$$R = \max_{\rho_{\mathbf{k}, \epsilon}} \sum_{\mathbf{k}, \epsilon} \frac{S(\rho_{\mathbf{k}, \epsilon})}{T} \cos \theta, \quad (30)$$

where θ is the polar angle of the mode wave vector \mathbf{k} and the maximum is performed over the mode states $\rho_{\mathbf{k}, \epsilon}$ (ϵ here counts the different polarizations of free-space electromagnetic waves). The presence of the term $\cos \theta$ is introduced in the sum to take into account the difference in the longitudinal speed of mode propagation. [In our calculation it is the nonlinear Eq. (2) that takes care of this.] Accordingly, the power constraint is calculated as

$$P = \sum_{\mathbf{k}, \epsilon} \frac{\text{Tr}[H_{\mathbf{k}, \epsilon} \rho_{\mathbf{k}, \epsilon}]}{T} \cos \theta. \quad (31)$$

This procedure assumes implicitly that the maximum communication rate is achieved by a global state of the input modes which is unentangled over \mathbf{k} . This assumption is correct as can be seen (at least for the waveguide communication protocol studied here) from the factorized form of the state in Eq. (9). In order to compare the two approaches, we have calculated the maximum rate of the waveguide using Eqs. (30) and (31) in place of Eqs. (7) and (4). The results are, predictably, similar to the ones reported in Sec. II A, even though the numerical factor differs: in fact, for multi-mode communication and high-power regime, we now find

$$R = \frac{4}{3 \ln 2} \left(\frac{g \pi^2 A}{120 c^2} \right)^{1/4} \left(\frac{P}{\hbar} \right)^{3/4} \quad (32)$$

smaller than Eq. (18) by a $(3/2)^{1/4}$ factor, which derives from the particular choice of maximization of Eq. (30).

If we consider the case of a single directional mode, on the other hand, R scales as $\cos \theta P^{1/2}$ [see Eq. (29)]: this is the same result obtained in the free-space propagation [1,2], apart from the $\cos \theta$ factor that takes into account the decrease in longitudinal propagation speed of the field due to the reflections at the waveguide walls.

All the results discussed in this paper have been obtained in the lossless case, in which all the photons injected into the waveguide arrive to the receiver. In the presence of loss, the calculation procedure complicates noticeably: the capacity is no more simply given by the entropy of the initial state, but by the Holevo quantity, which is not known to be additive over successive uses of the channel [6,9,10]. Finally, we have not considered the presence of prior entanglement shared between the sender and the receiver. In this case the rate R can be doubled by using the superdense coding protocol [11]. The calculation of the entanglement assisted capacity for the single directional mode case in the presence of loss was given in Ref. [12], following the procedure of Ref. [13].

In conclusion we have calculated the maximum communication rate for a perfect waveguide in the two regimes of multimode and single directional-mode communication. A comparison with the known results on free-space communication schemes has been given.

ACKNOWLEDGMENTS

This work was funded by the ARDA, NRO, NSF, and by ARO under a MURI program.

APPENDIX

In this appendix the integration needed for Eq. (15) is given.

After performing the change of variables $y_j = 2\lambda\hbar c x_j$ ($j = 1, 2, 3$), the integral in Eq. (15) becomes

$$\int_0^\infty dy_1 \int_0^\infty dy_2 \int_0^\infty dy_3 \ln \left[\frac{1}{1 - e^{-f(y)}} \right] \\ = \frac{\pi}{2} \int_0^\infty dx x \int_0^\infty dy \ln \left[\frac{1}{1 - e^{2x^2/(y - \sqrt{y^2 + 4x^2})}} \right], \quad (\text{A1})$$

where in the right-hand term polar coordinates have been employed in the (y_1, y_2) plane. Changing to polar coordinates also in the plane spanned by $(2x, y)$, the integral becomes

$$\int_0^{\pi/2} d\phi \frac{\pi \cos \phi}{(1 + \sin \phi)^3} \int_0^\infty dr r^2 \ln \left[\frac{1}{1 - e^{-r}} \right] = \frac{\pi^5}{120}. \quad (\text{A2})$$

-
- [1] C. M. Caves and P. D. Drummond, *Rev. Mod. Phys.* **66**, 481 (1994).
 [2] H. P. Yuen and M. Ozawa, *Phys. Rev. Lett.* **70**, 363 (1992).
 [3] D. Slepian, *J. Opt. Soc. Am.* **55**, 1110 (1965); H. P. Yuen and J. H. Shapiro, *IEEE Trans. Inf. Theory* **24**, 657 (1978).
 [4] M. Lachmann, M. E. J. Newman, and C. Moore, e-print cond-mat/9907500.
 [5] W. Greiner, *Classical Electrodynamics* (Springer, New York, 1998); H. A. Haus, *Electromagnetic Noise and Quantum Optical Measurements* (Springer, Berlin, 2000).
 [6] A. S. Holevo, *Probl. Inf. Transm.* **9**, 177 (1973).
 [7] A. S. Holevo, *IEEE Trans. Inf. Theory* **44**, 269 (1998); P. Hausladen, R. Jozsa, B. Schumacher, M. Westmoreland, and W. K. Wootters, *Phys. Rev. A* **54**, 1869 (1996); B. Schumacher and M. D. Westmoreland, *ibid.* **56**, 131 (1997).
 [8] J. D. Bekenstein, *Phys. Rev. D* **23**, 287 (1981); *Phys. Rev. A* **37**, 3437 (1988).
 [9] M. A. Nielsen and I. L. Chuang, *Quantum Computation and Quantum Information* (Cambridge University Press, Cambridge, 2000).
 [10] V. Giovannetti, S. Guha, S. Lloyd, L. Maccone, J. H. Shapiro, and H. P. Yuen, *Phys. Rev. Lett.* **92**, 027902 (2004).
 [11] C. H. Bennett and S. J. Wiesner, *Phys. Rev. Lett.* **69**, 2881 (1992).
 [12] V. Giovannetti, S. Lloyd, L. Maccone, and P. W. Shor, *Phys. Rev. Lett.* **91**, 047901 (2003); *Phys. Rev. A* **68**, 062323 (2003).
 [13] C. H. Bennett, P. W. Shor, J. A. Smolin, and A. V. Thapliyal, *IEEE Trans. Inf. Theory* **48**, 2637 (2002).